Journal of Building Engineering 32 (2020) 101526

Contents lists available at ScienceDirect

Journal of Building Engineering

journal homepage: http://www.elsevier.com/locate/jobe

Finite element modelling and parametric analysis of FRP strengthened RC beams under impact load

Majid M.A. Kadhim [a,*], Akram R. Jawdhari [b], Mohammed J. Altaee [c], Ali Hadi Adheem [d]

[a] College of Engineering, University of Babylon, Hilla, Iraq
[b] Department of Construction and Projects, University of Babylon, Hilla, Iraq
[c] Environment Research and Studies Center, University of Babylon, Hilla, Iraq
[d] Kerbala Technical Institute, Al-Furat Al-Awsat Technical University, 56001, Kerbala, Iraq

ARTICLE INFO

Keywords:
CFRP
Strengthening
Concrete beam
Finite element analysis
Impact load
ABAQUS
Debonding
Bond-slip

ABSTRACT

In this study, a non-linear three-dimensional finite element model was developed to study the impact behaviour of reinforced concrete beams strengthened in shear and/or flexure with carbon-FRP (CFRP) sheets. Concrete damage plasticity model was used for the concrete part, a traction-separation law for the CFRP-concrete interface, and Hashin criteria for rupture in CFRP. Comparisons with experimental data from literature, for various properties, confirmed the accuracy of developed model. A detailed parametric analysis was performed focusing on: the impact location as a ratio (α) from support to mid-span, impact velocity (v); and several geometrical properties related to CFRP technique. Increasing α from 0.26 to 0.79 results in increasing the maximum displacement (Δ_{max}) for both un-strengthened and strengthened beams. CFRP strengthening resulted in decreasing Δ_{max} for different values of α and v and prevented global concrete failure for $v = 8.86$ m/s. Δ_{max} is also decreased by 13% when a round corner and an arched soffit were used to prepare the beam substrate for bonding the transverse sheets instead of a sharp corner. Furthermore, the paper presents detailed discussions and implications for the above parameters and two additional ones, namely: configuration of transverse sheets (continuous wraps or discontinuous strips) and thickness of CFRP longitudinal sheets.

1. Introduction

As number of terrorism activities increased over the last two decades, it became imperative to protect human's lives and infrastructure from accidental loads by proper selection of construction materials and efficient rehabilitation methods [1]. Due to their superior properties and trusted performance [2,3], the use of fibre reinforced polymer (FRP) composites in repair and protection against impact and blast loads has increased numerously [4–8]. However, the durability consideration can limit the utilisation of FRP composites in various environments where carbon-FRP (CFRP) typically experiences galvanic corrosion, while the glass-FRP (GFRP) is not recommended in alkaline environment [9]. Many recent researches focused on the effects of blast and impact loads on structures [4,5], but few studies focused on FRP strengthened members [6–8,10–12]. In those available studies, carbon-FRP (CFRP) was the most investigated external reinforcement, likely due to its higher tensile strength.

One of the available researches on FRP retrofitted concrete beams under impact loads, is by Erki and Meier [6], which tested eight beams, having 8 m length and externally bonded by multiple layers of CFRP sheets. The impact load was applied by rising up one end of beam and dropping down on support. The results showed that CFRP reinforcement enhanced the beams' flexural strength and reduced their maximum deflection. White et al. [8] performed another experimental study on reinforced concrete (RC) beams under high loading rate after strengthening with CFRP laminates. Results revealed that the beams gained about 5% increase in strength and stiffness. They indicated also there is no change in the failure mode, initially being by flexure.

Tang and Saadatmanesh [7] presented another technique to apply the impact load, by dropping a steel cylinder onto the top face of the beam. CFRP composite was externally bonded to the top and bottom faces of the beam. The results revealed that the composite sheets can significantly improve the bending strength and the stiffness of the retrofitted RC beams, tested under impact. Furthermore, Soleimani, et al. [10] has also investigated experimentally the behaviour of RC beams, bonded with glass-FRP (GFRP) sheets, and subjected to quasi-static and

* Corresponding author.
E-mail address: eng.majid.mohammed@uobabylon.edu.iq (M.M.A. Kadhim).

https://doi.org/10.1016/j.jobe.2020.101526
Received 12 August 2019; Received in revised form 17 April 2020; Accepted 23 May 2020
Available online 2 June 2020

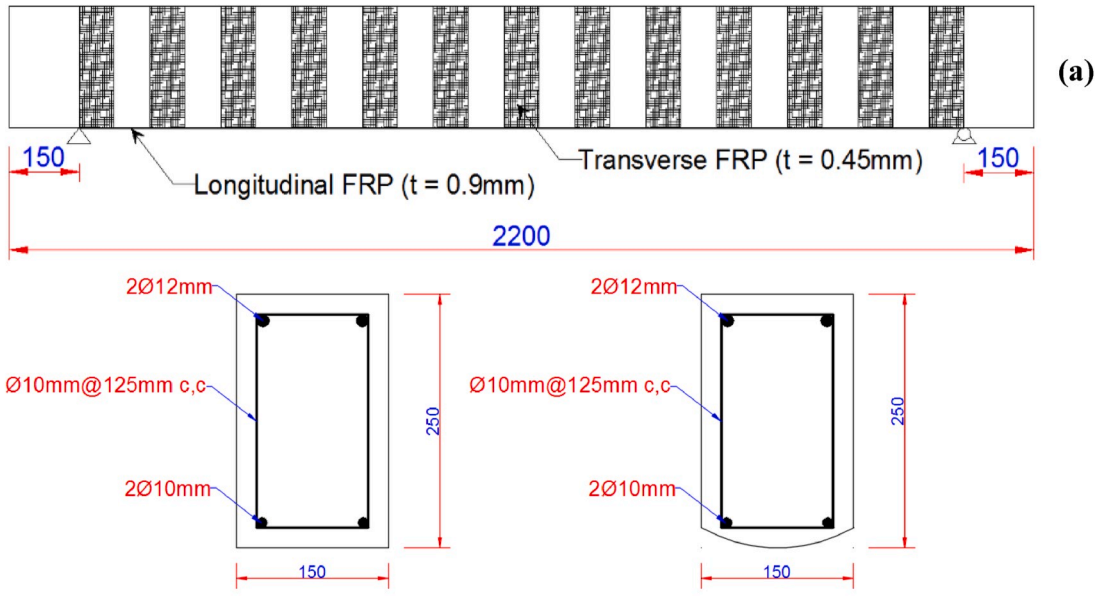

(b) Left: sharp corner [all beams, except ML2T7B], right: arched soffit [beam ML2T7B]

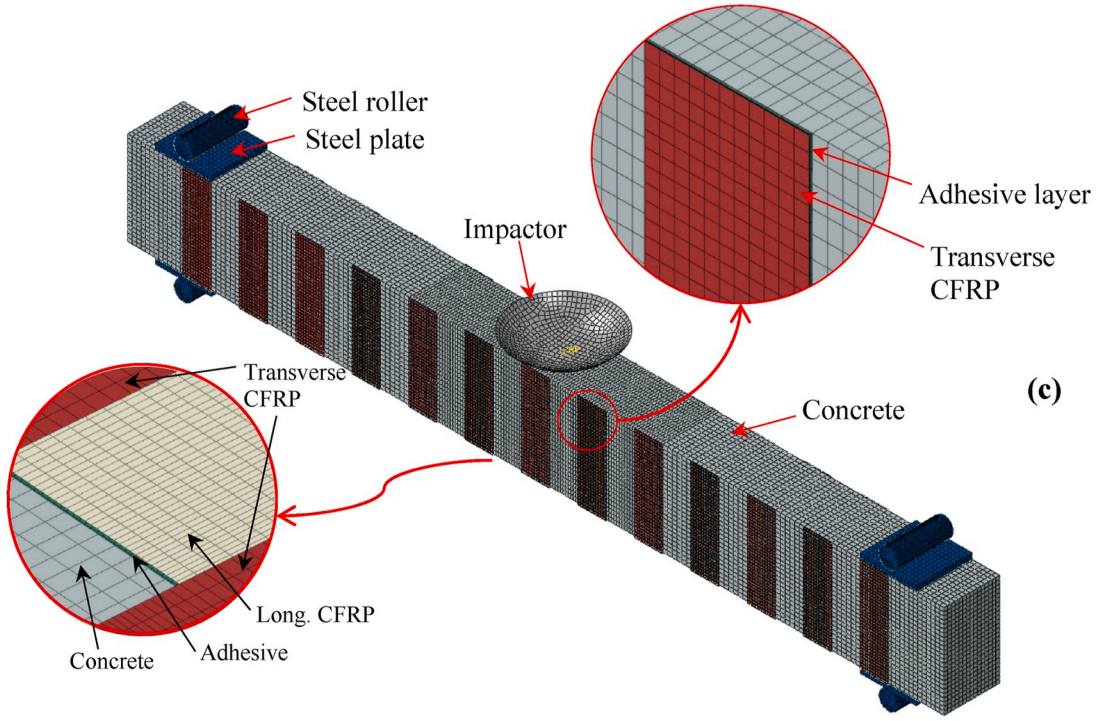

Fig. 1. CFRP-strengthened RC beams under impact, (a) side view, (b) cross-section, (c) 3D FE model.

impact loading conditions. Results also confirmed the viability of FRP technique in strengthening against such accidental loads.

In all of the above mentioned studies, the FRP was applied to improve the flexural capacity of the concrete beams. However, increasing the flexural strength can shift failure from ductile bending to brittle shear, particularly under impact loads [13,14]. Thus, Pham and Hao [11] took notice of this issue and included FRP shear reinforcement in the form of U-wraps and 45° angled wraps, in addition to the longitudinal CFRP sheets intended for upgrading the bending strength. Pham and Hao [11] reported significant stress concentrations at the sharp beam corners where the shear reinforcement is bonded and proposed rounding the beam soffit with a radius of 125 mm (modified section). The impact tests included seven beams; one un-strengthened, two strengthened using an arc soffit (modified section), and four also strengthened but with sharp beam corners. Results showed that rounding the corner significantly increases the beam's capacity as compared to no rounding, when comparing beams strengthened with the same amount of FRP reinforcement.

As research is still limited, investigation of FRP-strengthened RC members subjected to impact or blast loads is warranted, particularly on

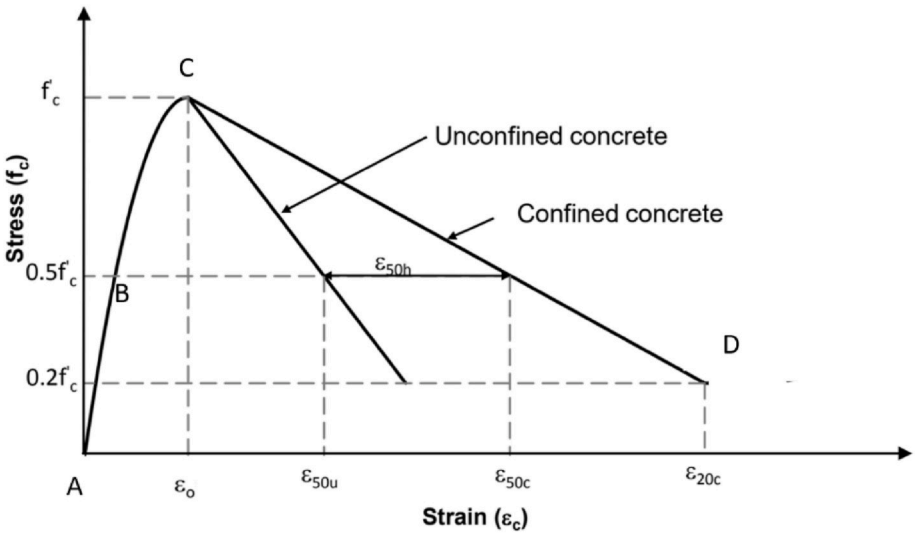

(a) Compression

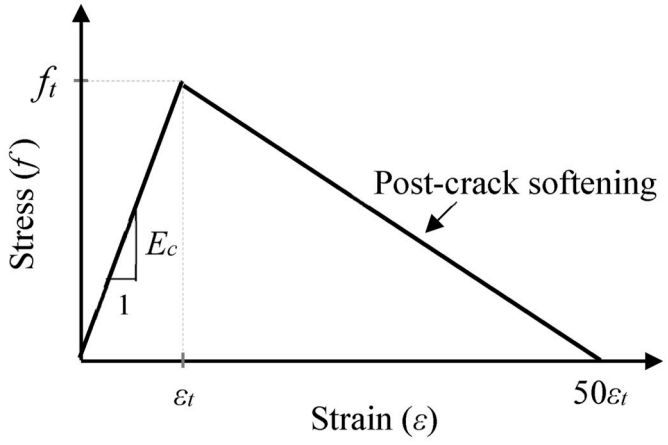

(b) Tension

Fig. 2. Implemented material stress-strain model for concrete beams.

Table 1
CDP concrete material parameters, based on ABAQUS recommendations.

Parameter	Value	Description[a]
Ψ	30	Dilation angle
∈	0.1	Eccentricity
fb_o/fc_o	1.16	The ratio of initial equibiaxial compressive yield stress to initial uniaxial compressive yield stress.
K	0.667	Kc, the ratio of the second stress invariant on the tensile meridian
μ	0.0001	Viscosity Parameter

[a] According to ABAQUS [15].

Table 2
Material properties of the CFRP reinforcement.

Property	Description	Unit	Value
ρ[a]	Density	Kg/m^3	1600
E_1	Elastic modulus in longitudinal (fiber) direction	GPa	89
E_2[b]	Elastic modulus in transverse (matrix) direction	GPa	17
G_{12}[a]	In-plane shear modulus	GPa	6
σ_{1t}[b]	Longitudinal tensile strength	MPa	1548
σ_{1c}[a]	Longitudinal compressive strength	MPa	1200
σ_{2t}[a]	Transverse tensile strength	MPa	50
σ_{2c}[a]	Transverse compressive strength	MPa	250
τ_{12}[a]	In-plane shear strength	MPa	70

[a] Property was obtained from Dolce [25].
[b] Property was obtained from testing by Pham and Hao [12].

the issue of shear failure. In addition, there is also a lack of finite element (FE) studies concerning this topic. FE analysis is a powerful and economical tool to investigate the response of structures under various loads and examine virtually endless number of variables that would be otherwise very difficult to be performed experimentally, due time, cost, and laboratory restraints. In this paper, a robust three-dimensional 3D FE model was developed and calibrated for RC beams strengthened with shear and flexural CFRP composites and subjected to impact load, comparing against several tests found in the literature. Proper modelling techniques were used for simulating the linear and nonlinear material

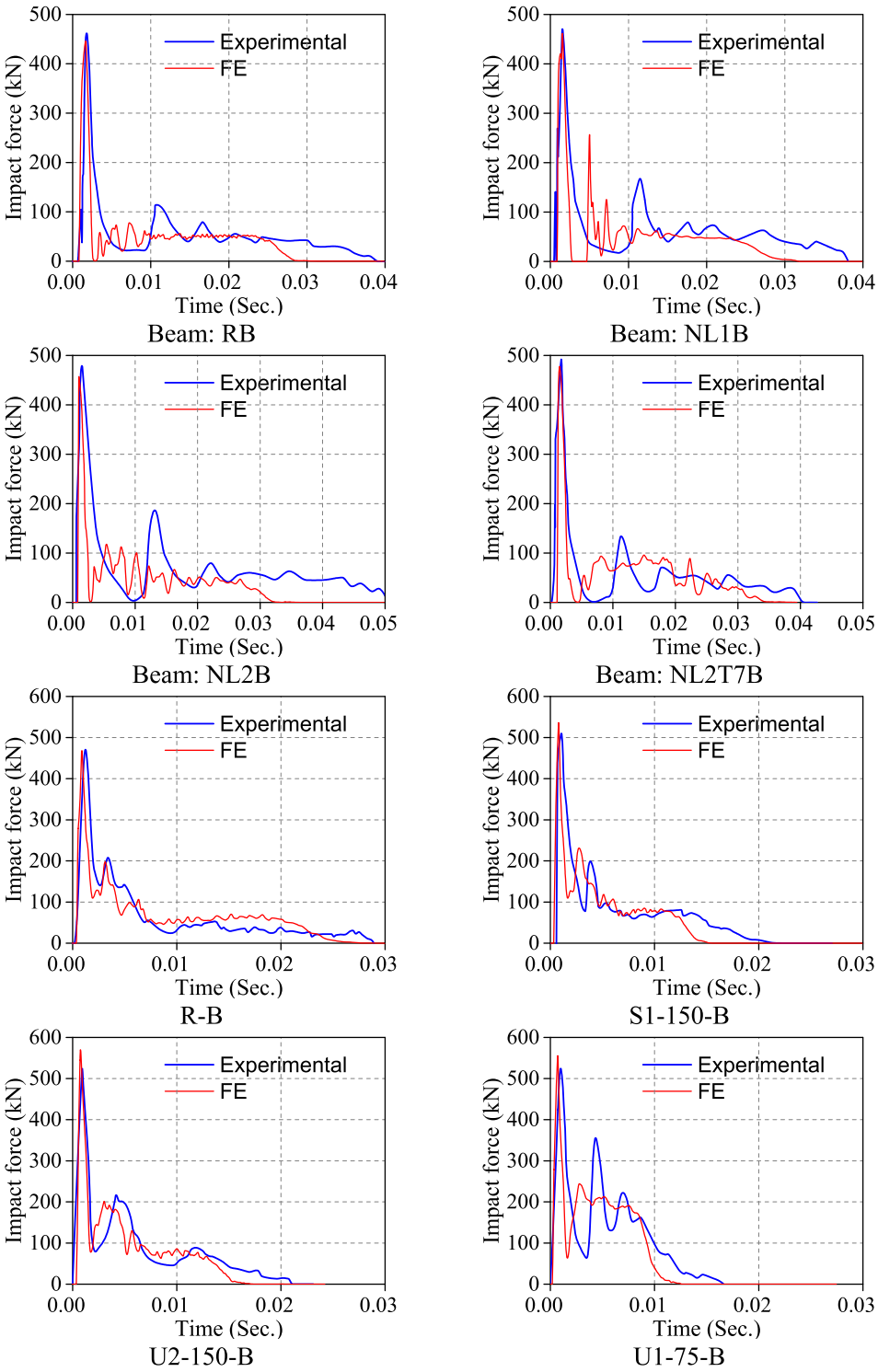

Fig. 3. Comparison of experimental and FE impact force-time histories.

properties, and FRP-concrete interfacial relations. The calibrated model was then used in a detailed parametric study, focusing on the effects of impactor location relative to mid-span, CFRP configuration, and impact velocity, among other parameters discussed in following sections.

2. Summary of experimental program

To validate the accuracy of developed FE models, two sets of experimental works were used, totalling eight samples. The first set contains a series of FRP strengthened beams in shear and flexure [12], while the second set includes four beams, three of were which strengthened in shear with various FRP configurations [11].

2.1. Pham and Hao [12] experiment

In this test, several un-strengthened and CFRP-strengthened RC beams tested under impact load by Pham and Hao [12] were tested. The rectangular beams had dimensions of 150 mm, 250 mm, and 2200 mm for the width, depth, and total length, respectively, with an effective span between supports of 1900 mm as shown in Fig. 1. The flexural and

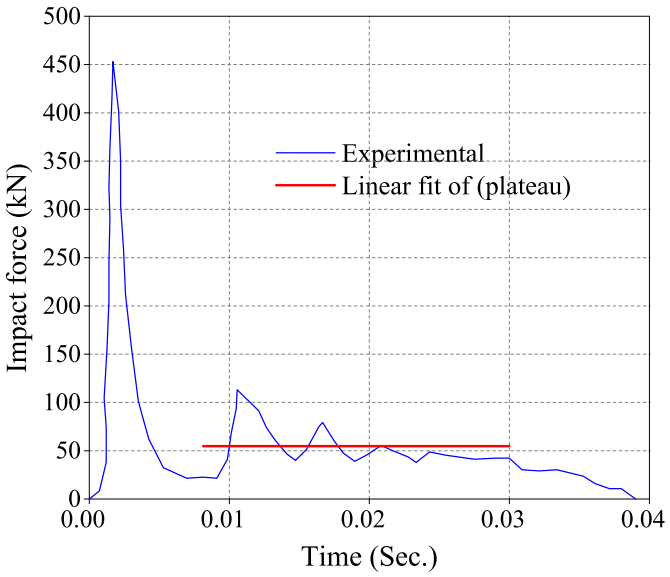

Fig. 4. Calculation of the plateau force for beam RB.

shear steel reinforcement consisted of two φ-10 mm deformed bars for longitudinal tension, φ-12 mm deformed bars for longitudinal compression, and φ-10 mm plain stirrups at 125 mm centre-to-centre spacing for shear. The yield strengths of the deformed and plain (cold formed) reinforcements were 500 and 250 MPa, respectively, while concrete compressive strength was 46 MPa.

The beams were strengthened for flexure and shear by externally bonded CFRP sheets, having a thickness (t_f) of 0.45 mm, and a width (b_f) of 75 mm. The tensile strength and elastic modulus of the composites were 1548 MPa and 89 GPa, respectively. Four samples were selected in this study for numerical modelling, including; un-strengthened sample as a reference beam (RB); two samples strengthened with one and two layers of CFRP sheets in the longitudinal direction (NL1B and NL2B respectively); and a forth sample strengthened with two layers of CFRP sheets in the longitudinal direction and 14 discontinuous CFRP U-wraps to mitigate shear failure. The impact tests were performed by dropping a mass, weighing a 203.5 kg, from a 2 m vertical distance into the beam's top face at mid-span, resulting in theoretical velocity of 6.28 m/s.

2.2. Pham and Hao [11] experiment

Similar to the previous experiment, the cross section dimensions in Pham and Hao [11] experiments were 150 mm × 250 mm but with a clear span length of 1100 mm. The beams were reinforced with flexural steel bars only, including two 12 mm bars in the compression side and two 16 mm bars in the tension side. The properties of all materials were identical to those in the previous experiment, except the concrete compressive strength was slightly higher at 47 MPa.

From the tested samples, four were selected in this study to validate the model simulations for FRP strengthened RC beams in shear, including one un-strengthened (beam R-B) and three strengthened beams, namely: beam (S1-150-B), strengthened with discontinuous side CFRP strips with a strip width (w) of 75 mm and spacing (s) between strips of 150 mm; beam (U2-150-B), strengthened with two layers of discontinuous CFRP U-wraps with w and of s 75 and 150 mm, respectively; and beam (U1-75-B) strengthened with one layer of continuous CFRP U-wrap.

3. Numerical modelling

3.1. Element types

The numerical beam models were generated using the general purpose FE software ABAQUS [15] utilizing the explicit dynamic solver. The concrete volume was meshed at 5 mm in size, and modelled by the eight-node brick element (C3D8R). A two-node linear displacement truss element (T3D2) was used to model the internal steel reinforcement (longitudinal and stirrups), which was assumed to be embedded in the concrete part. The impactor was modelled using a discrete rigid body with a reference point to provide the impacting mass. The CFRP sheet were modelled by the four-node shell element (S4R) [16,17]; while the connection between CFRP and concrete was simulated by an 8-node three-dimensional cohesive element (COH3D8) [15]. Brick element (C3D8R) was also used to model the steel plates and rollers shown in Fig. 1(b).

3.2. Material idealization

Concrete: the model proposed by Kent and Park [18], which is widely used for modeling confined concrete [3], is used in this study to model the RC beams with rectangular hoop confinement. The model, shown in Fig. 2(a), can be characterised by two portions; a parabolic ascending curve up to the concrete strength (fc'), and a linear descending line afterward up to failure. In the first portion, the concrete is assumed to be linear up to a stress of 0.5 $f_c^{'}$ [region AB in Fig. 2(a)]. The concrete stress (f_c) in the following region [line BC in Fig. 2(a)] is related to the concrete strain (ε_c) by Eq. (1):

$$f_c = f_c^{'}\left(2\left(\frac{\varepsilon_c}{\varepsilon_o}\right) - \left(\frac{\varepsilon_c}{\varepsilon_o}\right)^2\right) \quad (1)$$

where ε_0 is the strain at fc', and can be calculated as $\varepsilon_0 = \frac{2f_c^{'}}{E_c}$ [18], in which, E_c, is the concrete modulus, determined from ACI 318-14 [19] as [$E_c = 4700\sqrt{f_c^{'}}$]. For region CD in the second portion [i.e. at $\varepsilon_o \le \varepsilon_c \le \varepsilon_{20c}$], the f_c-ε_c relation is linear [Fig. 2(a)] with a slope

Table 3
Comparison of key results obtained from FE models and tests.

Beam	Max. displacement, Δ_{max} (mm)		% Diff.[a]	Residual displacement, Δ_R (mm)		% Diff.[a]	Max. force, $F_{max.}$ (kN)		% Diff.[a]	Duration, D (Sec.)		% Diff.[a]	Plateau, F_{pl} (kN)		% Diff.[a]
	Exp.	FE	%	Exp.	FE	%	Exp.	FE	%	Exp.	FE	%	Exp.	FE	%
RB	52.3	51.3	1.9	41.6	40.9	1.7	453	442	2.4	0.039	0.032	18	54.6	51.1	6.4
NL1B	41.1	41.6	1.2	31.2	31.1	0.2	470	461	1.9	0.038	0.032	16	64.5	61.1	5.3
NL2B	44.2	45.6	3.2	28.7	31.2	8.7	464	457	1.5	0.051	0.038	25	62.7	60.5	3.5
NL2T7B	39.5	38.1	3.5	29.8	29.1	2.3	492	464	5.7	0.040	0.034	15	70.8	73.2	3.4
R-B	37.2	36.6	1.6	28.0	27.7	1.1	457	468	2.4	0.029	0.027	7	44.6	46.3	3.8
S1-150-B	32.6	31.0	4.9	25.9	25.2	2.7	510	536	5.1	0.022	0.016	23	72.4	74.8	3.3
U2-150-B	28.9	27.8	3.8	21.3	20.8	2.3	524	544	3.8	0.022	0.017	18	67.5	72.7	7.7
U1-75-B	18.6	18.6	0.0	12.1	11.7	3.3	517	555	7.4	0.016	0.012	25	158.2	162.5	2.7

[a] $\%Diff. = \left(\frac{FE - Exp.}{Exp.}\right) \times 100$

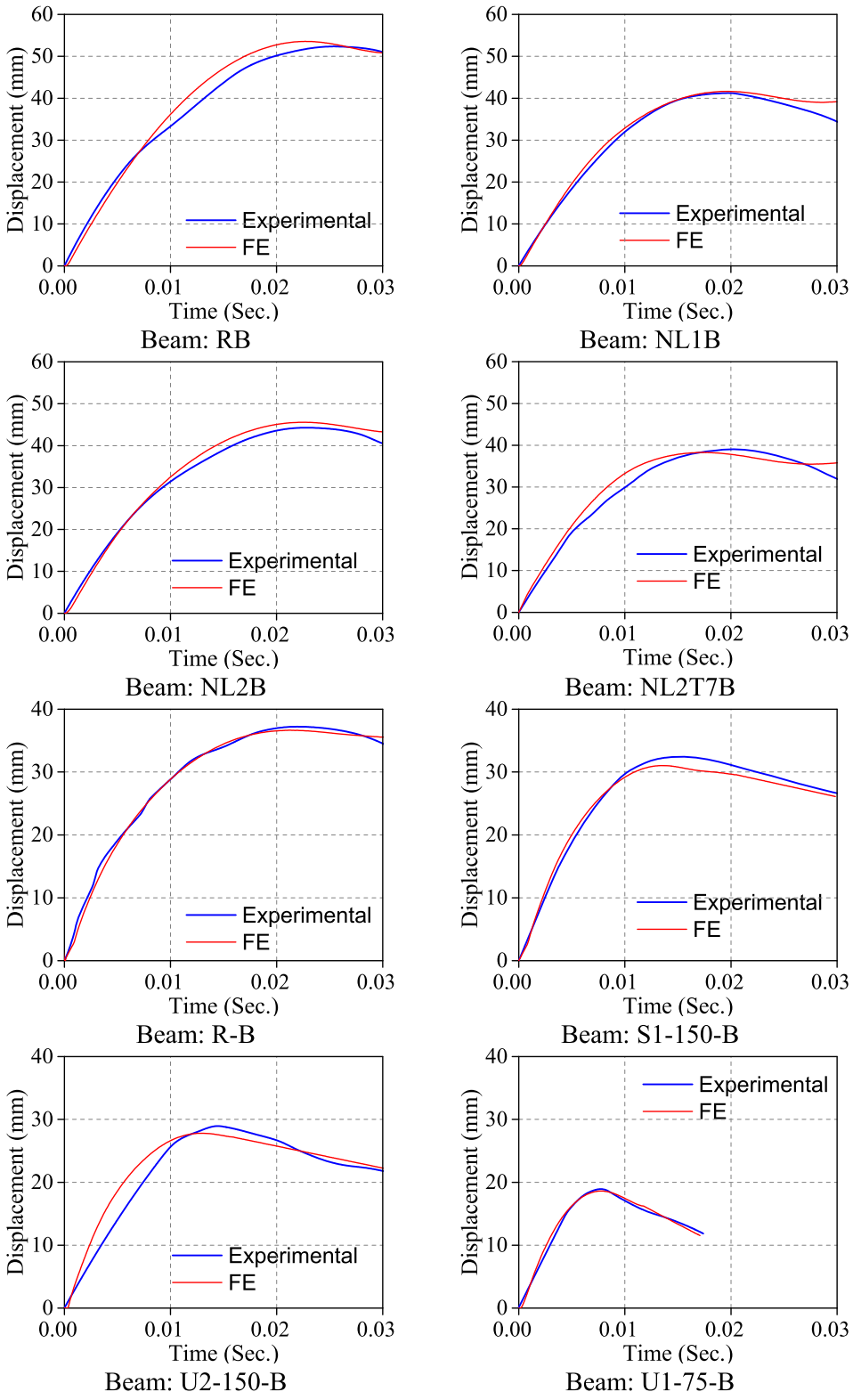

Fig. 5. Comparison of experimental and FE displacement-time histories.

governed by the confinement ratio, depending on the stirrup details as explained below:

$$f_c = f_c^{'}(1 - Z(\varepsilon_c - \varepsilon_o)) \quad (2)$$

Where

$$Z = \frac{0.5}{\varepsilon_{50u} + \varepsilon_{50h} - \varepsilon_{co}} \quad (3)$$

$$\varepsilon_{50u} = \frac{30 + 0.29 f_c^{'}}{145 f_c^{'} - 1000} \quad (4)$$

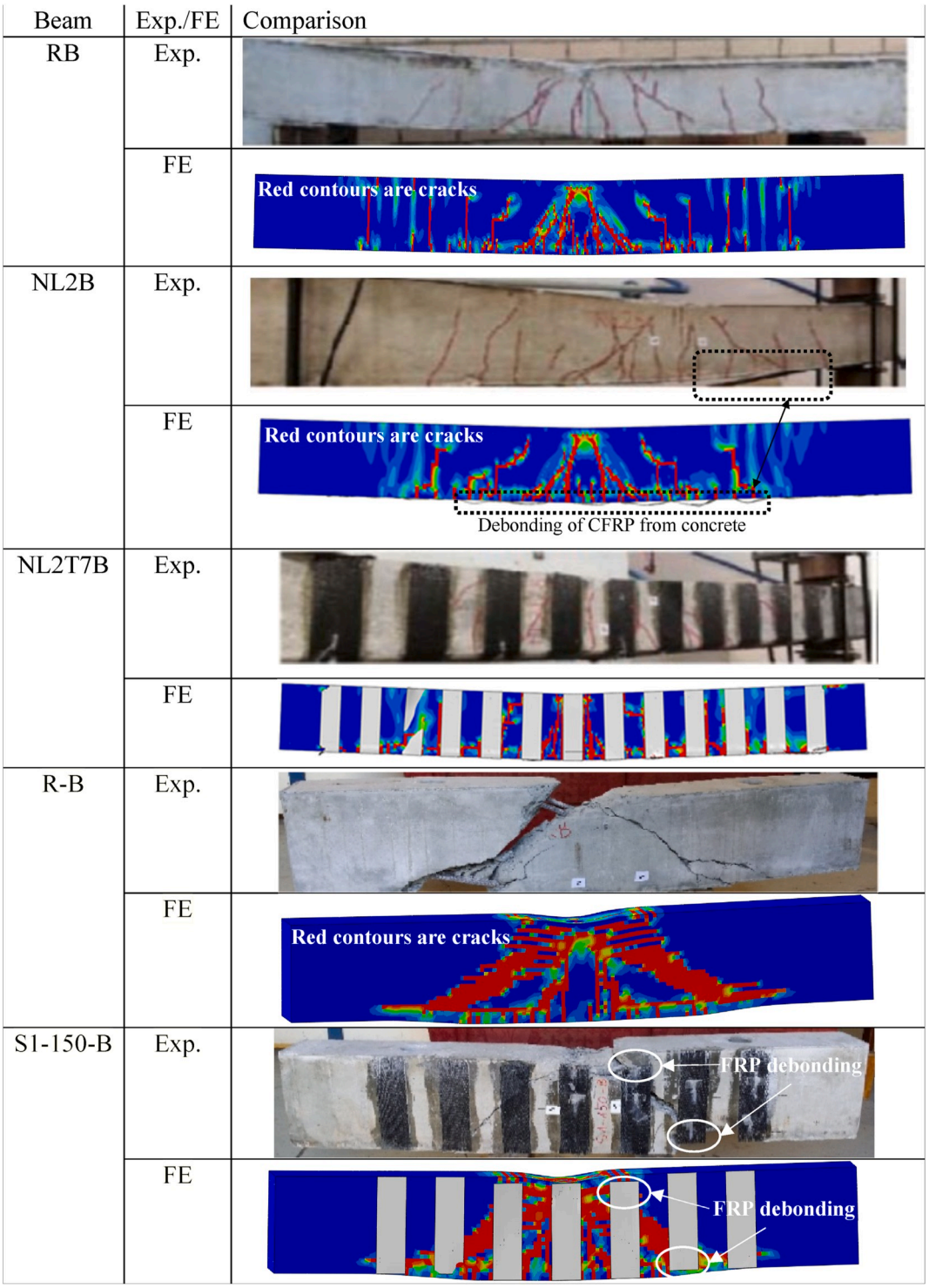

Fig. 6. Comparison of experimental and FE crack patterns and failure modes.

$$\varepsilon_{50h} = \frac{3}{4}\rho'' \sqrt{\frac{b''}{S}} \tag{5}$$

$$\rho'' = \frac{2(b'' + d'')A_s''}{b''d''S} \tag{6}$$

Where b'' and d'' are the width and depth of the confined core respectively, A_s'' is the cross-sectional area of the hoop bar and S is the centre-to-centre spacing of the hoops. In tension, a simple bilinear stress-strain curve is adopted with a peak stress corresponding to the concrete tensile strength according to ACI 318-14 [19] formula, and an ultimate strain of 50 times the strain at cracking [20], Fig. 2(b).

The above models (in tension and compression) were implemented within the framework of concrete damage plasticity (CDP), which is one of three approaches available in ABAQUS for simulating damage behaviour of brittle materials such as concrete. The other two approaches are: concrete smeared crack model, and brittle crack concrete model. In order to fully define CDP model, the parameters in Table 1 are required and their numerical values were selected based on recommendations of SIMULIA [15].

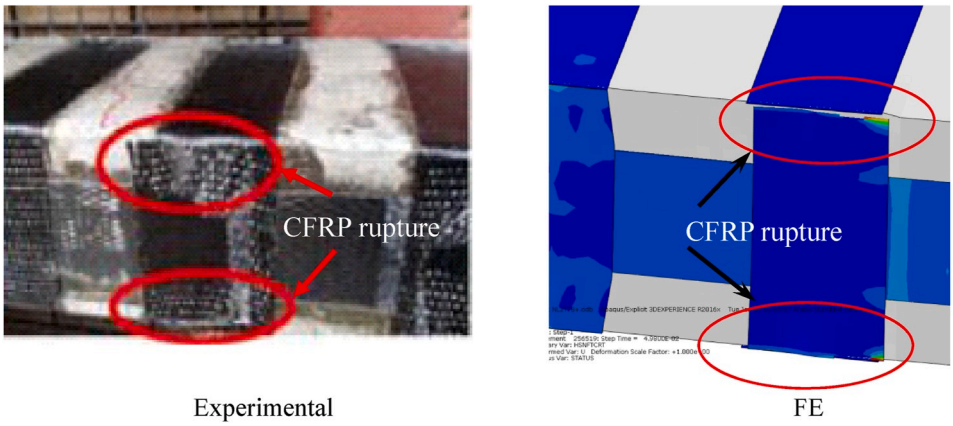

Fig. 7. FE simulation of rupture in CFRP U-wraps at corner, beam NL2T7B.

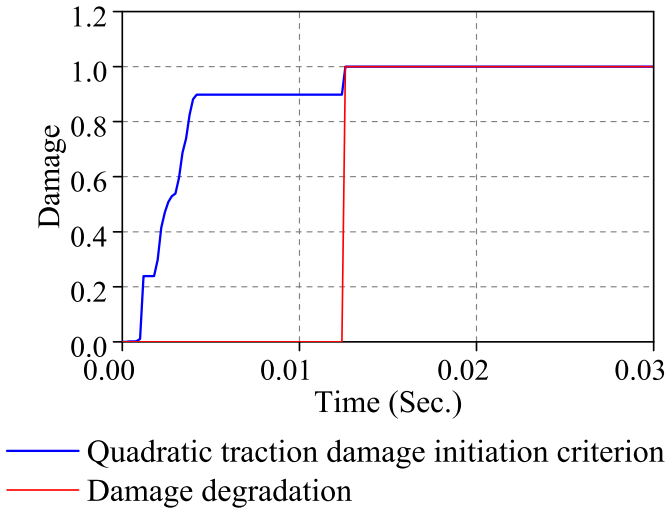

Fig. 8. Damage variables of epoxy at the mid-span of beam NL2T7B.

CDP model combines the theories of isotropic damaged elasticity along with isotropic tensile and compressive plasticity. It also assumes that the tensile cracking and compressive crushing are the two main failure mechanisms in concrete. The evolution of failure is controlled by tensile and compressive equivalent plastic strains under tension and compression loading, respectively. Damage parameters, d_t for tension and d_c for compression, with values ranging between 0 for undamaged state and 1.0 for complete damaged state, are introduced to control the evolution of damage and to degrade the material stiffness accordingly. Further explanation on CDP model can be found in ABAQUS documentation [15].

The effects of strain rate resulting from the impact load were considered by modifying the main inputs in the concrete stress-strain model, using the equations proposed by Fujikake [21] and reproduced bellow:

$$E_{0d} = E_0 \left(\frac{\dot{\varepsilon}}{\dot{\varepsilon}_{sc}}\right)^{0.002[log(\dot{\varepsilon}/\dot{\varepsilon}_{sc})]^{1.12}} \tag{7}$$

$$f'_{cd} = f'_c \left(\frac{\dot{\varepsilon}}{\dot{\varepsilon}_{sc}}\right)^{0.006[log(\dot{\varepsilon}/\dot{\varepsilon}_{sc})]^{1.05}} \tag{8}$$

$$\varepsilon'_{cd} = \varepsilon'_c \left(\frac{\dot{\varepsilon}}{\dot{\varepsilon}_{sc}}\right)^{-0.036+0.01\ log(\dot{\varepsilon}/\dot{\varepsilon}_{sc})} \tag{9}$$

Where E_{0d}, f'_{cd} *and* ε'_{cd} and E_0, f'_c *and* ε'_c represent the dynamic and static initial elastic modulus, compressive strength and the strain corresponding to the compressive strength respectively and $\dot{\varepsilon}_{sc} = 1.2 \times 10^{-5} 1/sec$.

Steel: the steel parts (reinforcement, rollers, and plates) were simulated as elastic-plastic material, using the classical metal plasticity model available in ABAQUS/Explicit. The strain rate effects in steel were considered, using Cowper-Symonds model [22], according to the following equation:

$$\dot{\sigma_0} = \sigma_0 \left[1 + \left(\frac{\dot{\varepsilon}}{D}\right)^{1/q}\right] \tag{10}$$

Where σ_o' is the dynamic flow stress at a uniaxial plastic strain rate of $\dot{\varepsilon}$, σ_o is the associated static flow stress, and D and q are constants for a given material. The values of these constants are 40.4 sec^{-1} and 5 respectively for mild steel [22,23].

CFRP sheet: an orthotropic linear elastic response was assumed for the CFRP sheet, whose main mechanical properties are shown in Table 2. The material failure due to either fibre modes (tension and compression), matrix modes, and inter-laminar shear, is discretely defined using Hashin's criteria [24], which is one of the well-known theoretical formula used to predict failure initiation and evolution in FRP composites. Five stress limits, related to each one of the above failure modes, are needed to define Hashin's criteria. These limits are listed in Table 2, and were either directly determined from tests by Pham and Hao [12] or obtained from other studies [25].

CFRP-concrete interface: a traction-separation law, commonly used to simulate the bond between CFRP and concrete or steel substrate [16,26,27], was used in this study to model the interaction between CFRP sheets and concrete, assuming slipping and debonding are due to cohesive failure in the adhesive layer. The model includes two stages that can be integrated in ABAQUS/Explicit solver; a linear elastic part, defined by the adhesive's elastic and shear moduli for the longitudinal and transverse directions; and damage stage, representing slippage initiation and propagation as well as complete separation. Lu et al. [28] bond-slip relation was used to simulate the FRP-concrete interface. It should be mentioned here that the bond-slip model suggested by Lu et al. [28] was proposed for quasi-static loading rates. However and due to limitations in the FE program (ABAQUS), this model is used in this study with impact loading rates. This kind of simplification was also found in the studies carried out on the strengthening of structures under impact loading rates such as [17,26,29].

4. FE results, validation and discussion

Fig. 3 shows the impact force-time history (*F-t*) curves, comparing

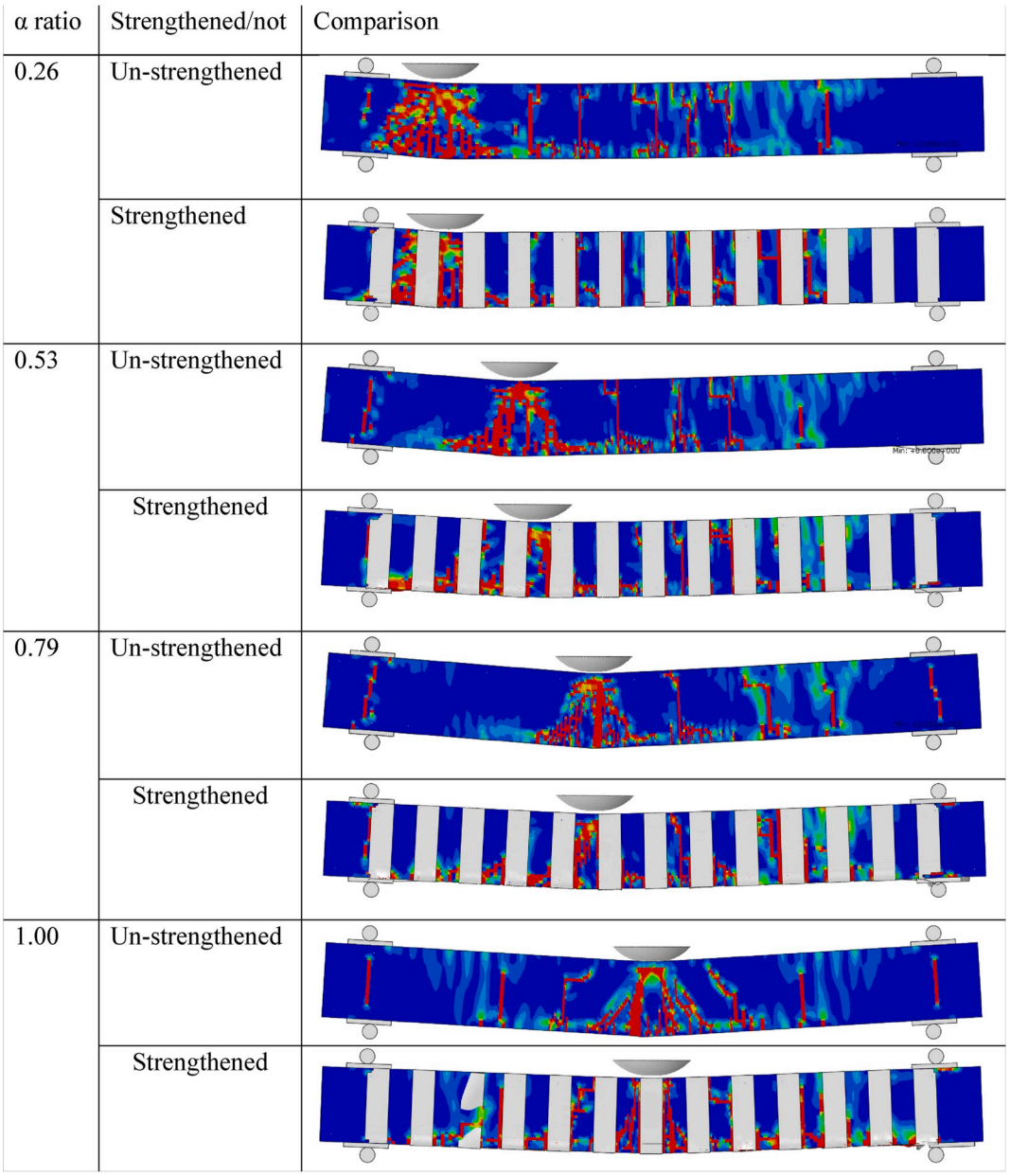

Fig. 9. Cracking patterns for different impact locations [α ratios], comparing un-strengthened and CFRP-strengthened RC beams.

experimental data and FE predictions, for the eight specimens selected from Pham and Hao [12] studies. The comparison demonstrates the capability of developed FE model in predicting the (*F-t*) curves of RC beams strengthened in shear and/or flexure under impact load, with reasonable accuracy. In addition to the general response, the model must be able to accurately predict the key points within the curve, which are (1) the maximum impact force ($F_{max.}$); (2) maximum displacement ($\Delta_{max.}$); (3) residual displacement ($\Delta_{R.}$); (4) plateau force (F_{pl}); (5) and impact duration (D). The last two parameters represent, respectively: the average impact force in the post-peak stage which can be calculated as shown in Fig. 4, and the overall period of the contact between the impactor and the specimen as defined in a previous research [30].

The FE predictions for $F_{max.}$, $\Delta_{max.}$, Δ_R and F_{pl} agreed very well with the experimental data, with a percentage difference of 1.5-7.4% for F_{max}, 0.0-4.9% for Δ_{max}, 0.2-8.7% for Δ_R and 2.7-7.7% for F_{pl}. More pronounced percentage deference between model and test, ranging between 7 to 25%, was noticed for the predictions of impact duration (D), as seen in Table 3. This could be due to: a variation of fixity conditions in the actual test which can't be captured numerically, the damping force introduced by the testing rig, model limitations in terms of material idealization and mesh, or a combination thereof. However, the observed difference in D is within the acceptable maximum range found in literature, for example 26% in Zeinoddini et al. [31], and doesn't affect the overall accuracy of the model results.

The displacement-time histories (Δ-t) for the modelled beams are plotted in Fig. 5. It can be noted from this figure that the strengthened beams usually have maximum displacement less than the un-strengthened beam, with different values based on the CFRP configuration. In addition, the comparison between the FE and experimental (Δ-t) history confirmed the capability of developed models in capturing these curves very well, for both, the un-strengthened samples, and those strengthened by longitudinal, longitudinal/transverse and transverse CFRP sheets. Furthermore, strengthening with CFRP can be regarded as an effective method to mitigate against impact and blast loads, as can be evidenced by the experimental results in Table 3 which shows a decrease in $\Delta_{max.}$ of 12.4 to 50.0% and an increase in F_{max} of 2.4 to 14.7%; when

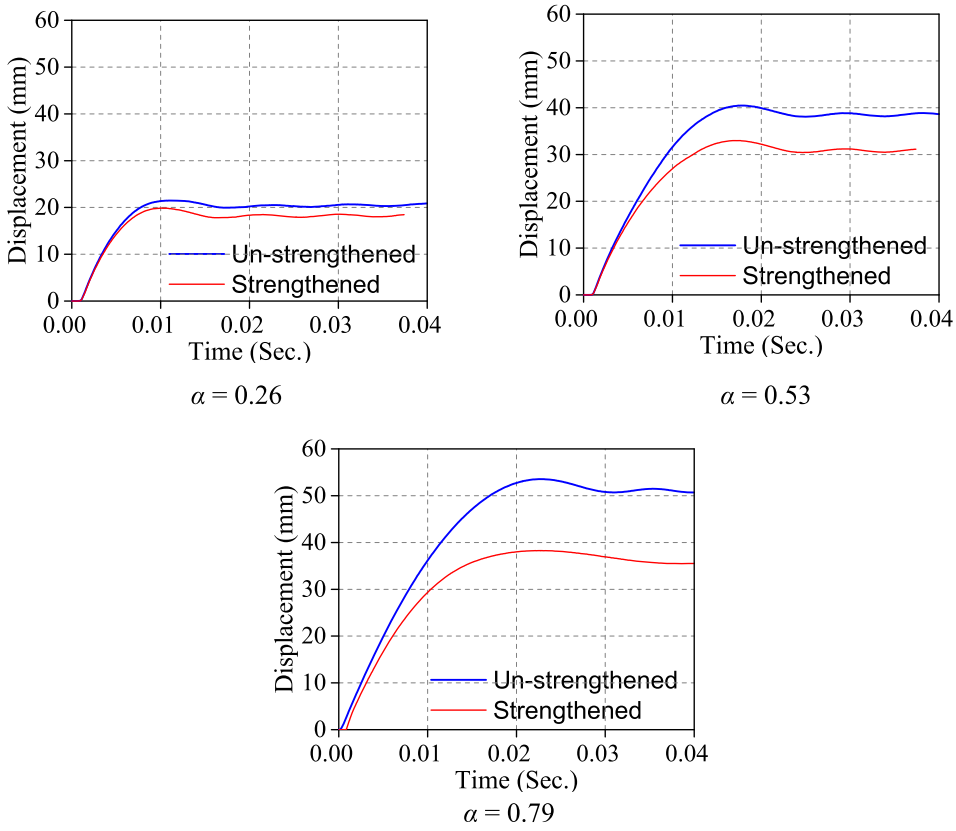

Fig. 10. Displacement-time histories of un-strengthened and CFRP-strengthened RC beams with various impact locations.

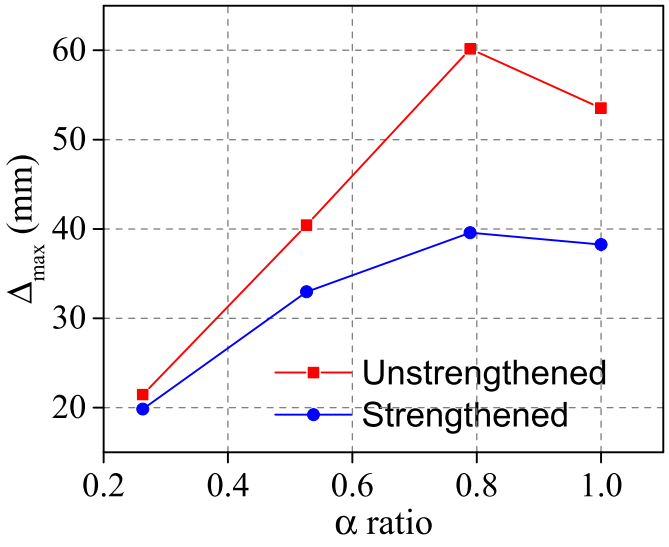

Fig. 11. Maximum displacement ($\Delta_{max.}$) vs. impact location [α ratios], comparing un-strengthened and CFRP-strengthened RC beams.

comparing strengthened specimens with the un-strengthened ones.

The concrete crack pattern is another way of validating the accuracy of a developed model. Typically, the cracking patterns are visualized in ABAQUS by plotting the concrete principal strains [32]; but in this study, a more accurate methodology is used by activating and plotting the tensile damage parameter (d_t) in the CDP model. Fig. 6 shows the experimental and FE predicted cracks patterns for three representative beams from the first experiment set [12] and two from the second set [11]. All beams in the first experiment had multiple shear–flexure cracks, even though the un-strengthened beam was designed to carry a static shear capacity of four times that in flexure. These cracks could be due to dynamic effects from the impact load [12].

The crack patterns from the model [Fig. 6], were almost identical to those occurring in the tests, confirming the accuracy of developed model. It can be seen from Fig. 6, for both experimental and model observations, that beam NL2B (strengthened with two layers of longitudinal CFRP) is having more shear cracks than un-strengthened sample (beam RB). This might be due to the additional flexural capacity observed in NL2B caused by applying two layers of longitudinal CFRP, resulting in activation of more cracks. Applying CFRP U-wraps, as in beam NL2T7B, didn't prevent the formation of shear cracks, but it decreased their widths significantly. Similarly, comparing the results of second experiment set with the FE results showed that the FE model was able to capture the predominant shear failure in all beams with good level of accuracy. In addition, the secondary failure mode by debonding of transverse CFRP strips which appeared in some beams such as beam S1-150-B was also correctly captured by the FE modelling, as can be seen in Fig. 6.

CFRP debonding and rupture were reported in several specimens in the experimental work of Pham and Hao [12]. Beam N1LB and NL2B, which were strengthened with one and two longitudinal CFRP sheets, respectively, experienced debonding of CFRP from concrete soffit. Fig. 6 shows the FE simulations of debonding, corresponding well with experimental observations. For beam NL2T7B, rupture of several CFRP U-wraps took place experimentally, probably due to stress concentrations as a result of the sharp corners. The CFRP rupture was accurately predicted by the Hashin's criteria in the numerical simulation, as seen in Fig. 7. Following the wrap rupture, debonding of longitudinal sheets also occurred experimentally and accurately simulated numerically by the traction-separation interfacial relation. Fig. 8 shows the damage variable in the epoxy layer at mid-span of beam NL2T7B, against time (t). The variable was zero initially indicating no debonding condition, but

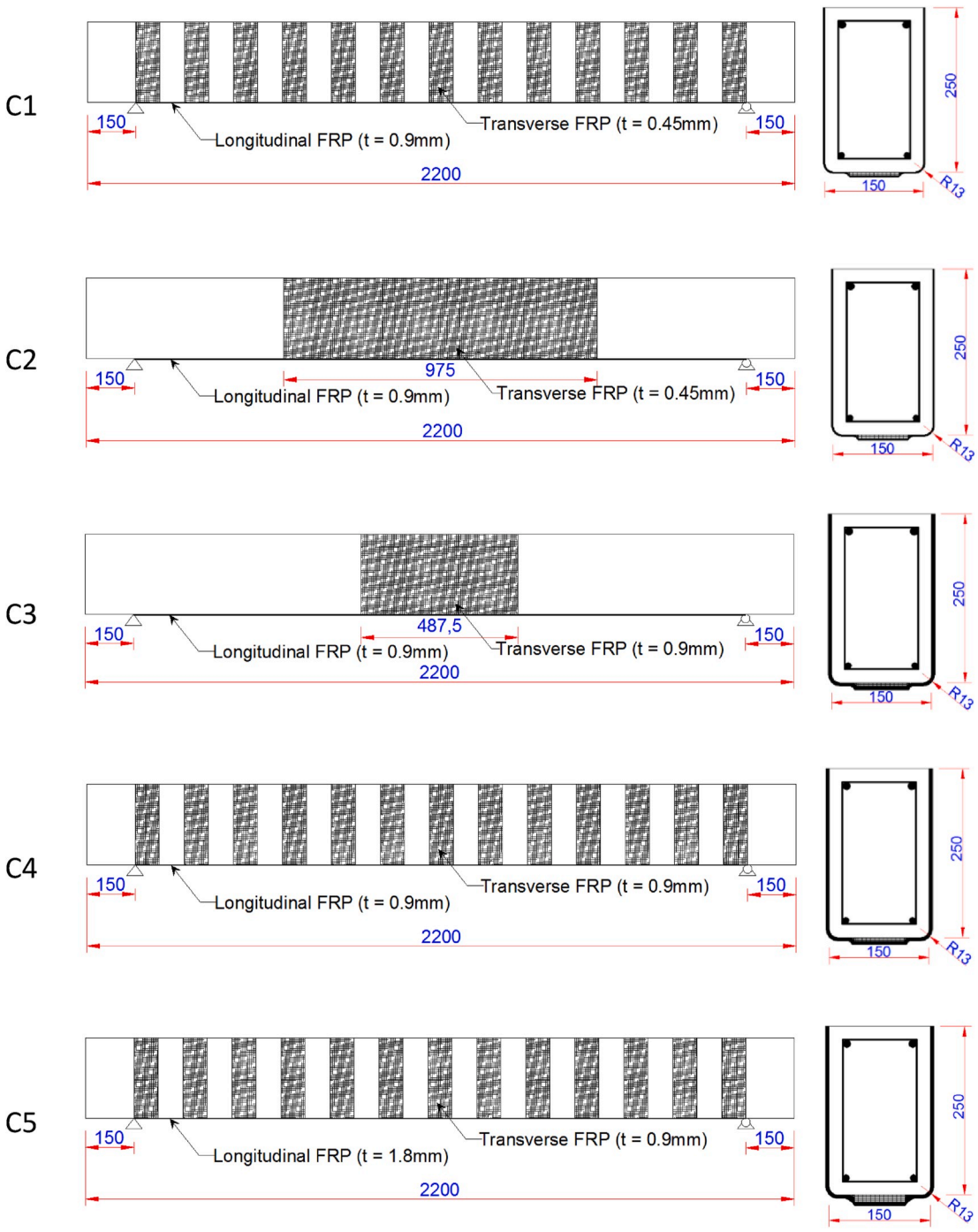

Fig. 12. Geometry of additional models, used in investigating effects of CFRP configuration.

increased gradually with time, and then attained a value of 1.0 at t = 0.125 s, indicating debonding at this instance.

5. Parametric study

Given the limited number of available studies on RC beams strengthened in shear and/or flexure and tested by impact loading, the calibrated FE model provides an excellent opportunity to examine in depth the behaviour of these members and carry out a detailed parametric analysis on the effects of several variables expected to affect the member's capacity. The following sections discuss the parametric analysis carried out on impact location and velocity, strengthening configuration and amount, and effects of beam corner treatment.

5.1. Impact location

The effects of impact location on the behaviour of CFRP-strengthened RC members under impact loads has not been investigated yet, thus it is included in the current parametric analysis. This factor was studied by varying the impact location as a ratio (α) relating the distance of the impactor from the left support (x) to half the span length ($L/2$) [$\alpha = x/(L/2)$]. Four values were chosen for α, 0.26, 0.53, 0.79, and 1.0 which is the original case in the validation models. Beam NL2T7B (strengthened with two longitudinal sheets in addition to transverse wraps) was selected to examine this parameter, in addition to the control beam (RB) which was used as a reference to examine the effectiveness and contribution of FRP strengthening.

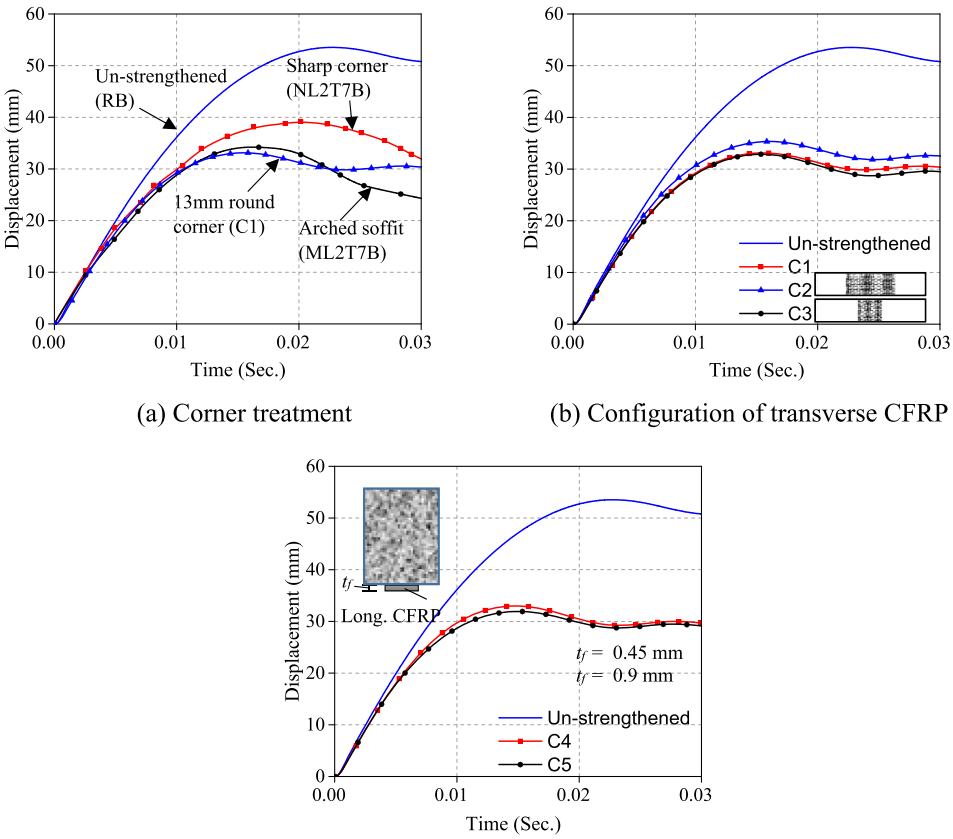

Fig. 13. Effects of various CFRP geometrical parameters on displacement-time histories.

Fig. 9 shows the crack patterns for the un-strengthened and strengthened models with different values for α. As can be seen, the CFRP strengthening, particularly the U-wraps, was very effective in reducing the intensity of cracks at failure. Fig. 10 plots the displacement-time (*D-t*) histories for α = 0.26, 0.53, and 0.79, considering both the un-strengthened and strengthened cases; in addition to the (*D-t*) curve for α = 1.0 which was already plotted in Fig. 5. In Fig. 11, the relations between maximum displacement within the (*D-t*) histories [$\Delta_{max.}$] and α ratio for strengthened and un-strengthened beams are presented. Results show that $\Delta_{max.}$ increases almost linearly, by 272% for un-strengthened cases and by 200% for strengthened ones, α when increases from 0.26 to 0.79. At α = 0.79 to 1.0, $\Delta_{max.}$ either decreased by 10% for un-strengthened cases or by 5% for strengthened ones. The increase of Δ_{max} as the impactor is moving away from support and closer to the mid-span, is expected and had previously been confirmed by Kadhim et al. [33] for CFRP-strengthened steel sections.

Examining the effectiveness of CFRP technique in strengthening RC beams under impact load, by comparing $\Delta_{max.}$for strengthened and un-strengthened samples in Fig. 11, it can be observed that the technique resulted in reducing Δ_{max} by 33% when α was 0.79 [impactor is 750 mm from support], and by 30% when α was 1.0 [impactor at mid-span]. The CFRP contribution then decreased gradually from 33% to 5%, when α decreased from 0.79 to 0.26. This is probably because Δ_{max} is at its highest value when the impactor is near or at mid-span (i.e. α→1.0]; therefore, adding CFRP flexural reinforcement in this case would increase the member's stiffness and reduce displacement more than if the impactor was near the support, in which case, Δ_{max} is already small before strengthening. In addition, as the impactor moves closer to the support, a strut will likely to form in concrete between the impactor and support. Fig. 9 shows the formation of the strut in the un-strengthened and CFRP strengthened models for α = 0.26, evidenced by the inclined shear cracks. Because of their low compressive strength and tendency to debond or buckle, CFRP U-wraps are not expected to provide a substantial resistance to the strut action.

5.2. CFRP geometrical parameters

Additional numerical models were generated to study the effects of three important geometrical parameters related to the CFRP reinforcement; corner treatment, configuration of transverse U-wraps, and thickness (t_f) of longitudinal sheets. Fig. 12 shows the geometry of constructed models. One issue that was noticed in both the experimental study of Pham and Hao [12] and FE model was the premature rupture failure of transverse wraps at the sharp corner between the beam's web and soffit, Fig. 7. In order to mitigate this failure, two additional models were created: C1— with a 13 mm round corner, see Fig. 12, recommended by ACI 440 committee [34]; and ML2T7B— with an arched soffit, see Fig. 1(b), recommended by Pham and Hao [12].

Fig. 13 (a) shows the (*D-t*) histories for different corner conditions, in addition to the numerical model of un-strengthened beam. As can be seen, using either the 13 mm round corner or an arched soffit resulted in a comparable 13% decrease of maximum displacement (Δ_{max}) compared to the model containing a sharp corner. The failure mode was also changed to rupture of longitudinal sheets, which provides a much better utilisation of CFRP material.

The effects of transverse wrap's geometry were examined by considering two commonly used configurations, continuous wraps or discontinuous strips. Three models were constructed: C1— having discontinuous strips identical to those in beam NL2T7; C2— having continuous wrap with a length of 975 mm [or 50% of total span]; and C3— having continuous wrap with a length of 487.5 mm [or 25% of total span]. All the three beams were designed with 13 mm round

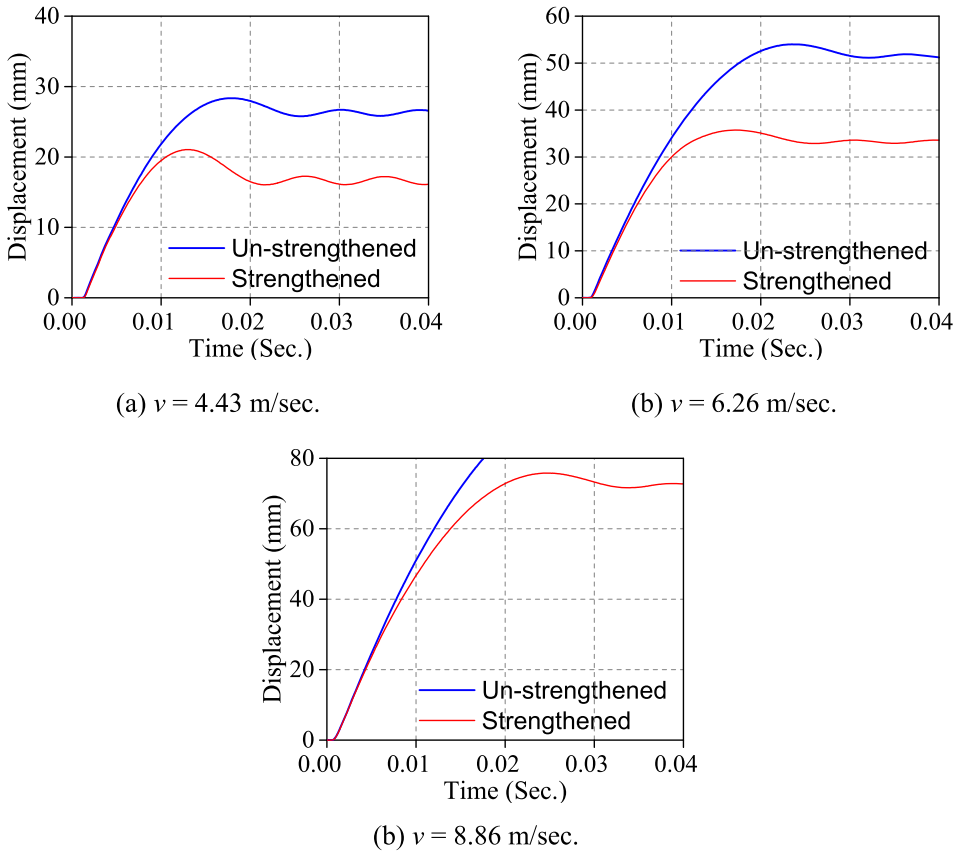

Fig. 14. Displacement-time histories of un-strengthened and CFRP-strengthened RC beams with various impact velocities.

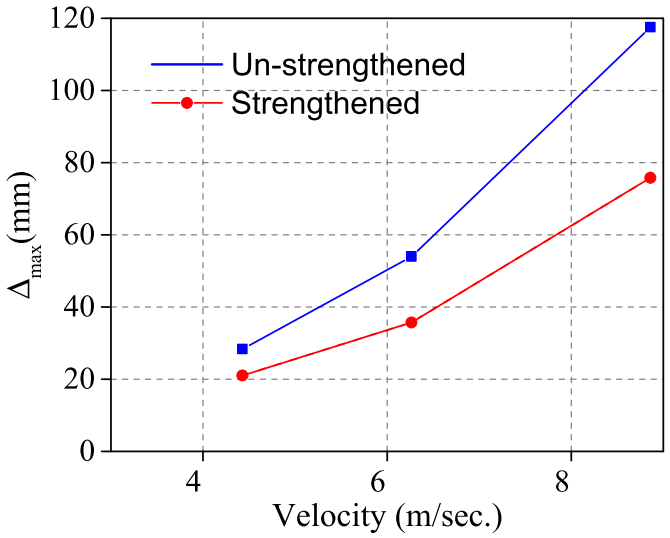

Fig. 15. Maximum displacement ($\Delta_{max.}$) vs. impact velocity, comparing un-strengthened and CFRP-strengthened RC models.

corner, as seen in Fig. 12. Fig. 13 (b) plots the (*D-t*) histories for the three beams along with the un-strengthened model. The three examined configurations resulted in a similar reduction of Δ_{max} by approximately 37%, compared to the un-strengthened sample, Fig. 13 (b), with a similar crack patters at mid-span region. Given the above result, it might be more practical and economical to use the continuous configuration of beams C2 or C3 in field applications.

Fig. 13 (c) shows the effects of (t_f) on the (*D-t*) histories, by comparing the response of three models, un-strengthened beam, strengthened with $t_f = 0.45$ mm [model C4 in Fig. 12], and strengthened with $t_f = 0.9$ mm [model C5 in Fig. 12], all having 13 mm round corner as discussed previously. The figure shows that doubling t_f caused a negligible improvement in the CFRP contribution to impact resistance, probably because failure was due to concrete cover separation which is not affected by thickness of CFRP but by concrete's tensile and shear strengths, as explained by Jawdhari et al. [2]. The reduction in Δ_{max} for both t_f values was approximately, 40% compared to the control model.

5.3. Impact velocity

The effects of impact velocity (v) on the behavior of CFRP-strengthened RC beam under impact load was investigated by using three values for v, 4.4, 6.26, and 8.86 m/s. Model C1, which is shown in Fig. 12 and discussed in the previous section, was selected as the strengthened model and compared with un-strengthened counterpart. Fig. 14 plots (*D-t*) histories for C1 and control models, for the three chosen velocities; while Fig. 15 shows the relation between Δ_{max} and v for the same samples.

Comparing the strengthened model with the control counterpart, Δ_{max} decreased by 26, 35, and 34%, for $v = 4.43$, 6.26, and 8.86 m/s, respectively. This shows that FRP technique can significantly improve the beam's resistance to impact, at various impact energy values. It was also noticed that at $v = 8.86$ m/s, the un-strengthened model experienced global failure under the impactor and was unable to absorb the impact energy. On the other hand, the CFRP-strengthened model successfully withstood the high velocity impact and didn't experience the global failure, showing great ductility. This important finding signifies the advantages of applying CFRP technique in retrofitting structures prone to accidental and dynamic loads such as earthquakes, vehicular impacts, and avalanches.

6. Conclusions

The use of carbon fibre-reinforced polymeric (CFRP) composites in strengthening or repairing reinforced concrete (RC) structures against service loads and accidental ones, such as impact and earthquakes, has become an effective and economical option. This paper examines the effects of transverse impact load on CFRP-strengthened RC beams, using a robust three-dimensional finite element simulation. Concrete material nonlinearity, rupture of CFRP, slipping and debonding from concrete were all included in the developed models. A detailed parametric study was also performed. The following conclusions were extracted based on the results of this investigation:

1 The developed model was found to give good predictions for CFRP-strengthened RC beams under impact; where numerical-to-experimental difference was 1.5-5.7% for maximum impact force, 1.2-3.5% for maximum deflection (Δ_{max}), and 3.4-6.5 for impact duration. The model was also able to accurately simulate CFRP rupture, debonding, and crack patterns.
2 The impact location as a ratio (α) from support to mid-span was varied from 0.26 to 1.0. It was found that Δ_{max} of un-strengthened and CFRP strengthened beams increased significantly when α increases from 0.26 to 0.79. CFRP strengthening has significant effects on reducing Δ_{max}, particularly for large α.
3 CFRP strengthening contributed almost equally in reducing Δ_{max} by an average of 32% when the impact velocity (v) was varied from 4.43 to 8.86 m/s. At $v = 8.86$ m/s, the CFRP reinforcement prevented a global concrete failure under the impactor occurring in the un-strengthened sample.
4 Corner treatment, by rounding or using an arched soffit, resulted in prevention of rupture in transverse CFRP sheets, and 13% decrease in Δ_{max}, relative to the model with sharp corner.
5 Configuration of transverse sheet, by using continuous wraps or spaced strips, results in a similar reduction of Δ_{max} by approximately 37%, compared to the control beam.

Declaration of competing interest

The authors declare that they have no known competing financial interests or personal relationships that could have appeared to influence the work reported in this paper.

CRediT authorship contribution statement

Majid M.A. Kadhim: Conceptualization, Methodology, Software, Validation, Investigation, Supervision. **Akram R. Jawdhari:** Writing - review & editing, Data curation, Investigation. **Mohammed J. Altaee:** Writing - original draft, Data curation, Writing - review & editing. **Ali Hadi Adheem:** Visualization, Writing - original draft.

Appendix A. Supplementary data

Supplementary data to this article can be found online at https://doi.org/10.1016/j.jobe.2020.101526.

References

[1] J. Li, C. Wu, H. Hao, An experimental and numerical study of reinforced ultra-high performance concrete slabs under blast loads, Mater. Des. 82 (2015) 64–76.
[2] A. Jawdhari, A. Peiris, I. Harik, Experimental study on RC beams strengthened with CFRP rod panels, Eng. Struct. 173 (2018) 693–705.
[3] A. Jawdhari, I. Harik, Finite element analysis of RC beams strengthened in flexure with CFRP rod panels, Construct. Build. Mater. 163 (2018) 751–766.
[4] K.-H. Min, J.-M. Yang, D.-Y. Yoo, Y.-S. Yoon, Flexural and punching performances of FRP and fiber reinforced concrete on impact loading, in: Advances in FRP Composites in Civil Engineering, Springer, 2011, pp. 410–414.
[5] T.M. Pham, M.N. Hadi, J. Youssef, Optimized FRP wrapping schemes for circular concrete columns under axial compression, J. Compos. Construct. 19 (6) (2015), 04015015.
[6] M. Erki, U. Meier, Impact loading of concrete beams externally strengthened with CFRP laminates, J. Compos. Construct. 3 (3) (1999) 117–124.
[7] T. Tang, H. Saadatmanesh, Behavior of concrete beams strengthened with fiber-reinforced polymer laminates under impact loading, J. Compos. Construct. 7 (3) (2003) 209–218.
[8] T.W. White, K.A. Soudki, M.-A. Erki, Response of RC beams strengthened with CFRP laminates and subjected to a high rate of loading, J. Compos. Construct. 5 (3) (2001) 153–162.
[9] L. Hollaway, A review of the present and future utilisation of FRP composites in the civil infrastructure with reference to their important in-service properties, Construct. Build. Mater. 24 (12) (2010) 2419–2445.
[10] S. Soleimani, N. Banthia, S. Mindess, Behavior of RC beams under impact loading: some new findings, in: Proceedings of the Sixth International Conference on Fracture Mechanics of Concrete and Concrete Structures, Catania, Italy, Taylor & Francis, London, 2007.
[11] T.M. Pham, H. Hao, Impact behavior of FRP-strengthened RC beams without stirrups, J. Compos. Construct. (2016), 04016011.
[12] T.M. Pham, H. Hao, Behavior of fiber-reinforced polymer-strengthened reinforced concrete beams under static and impact loads, Int. J. Prot. Struct. 8 (1) (2017) 3–24.
[13] S.F. Saatci, J. Vecchio, Effects of Shear Mechanisms on Impact Behavior of Reinforced Concrete Beams, American Concrete Institute, 2009.
[14] S.F. Saatcı, J. Vecchio, Nonlinear Finite Element Modeling of Reinforced Concrete Structures under Impact Loads, American Concrete Institute, 2009.
[15] SIMULIA, Analysis User's Manual. Providence, Rhode Island, USA, SIMULIA, Dassault Systèmes, 2016.
[16] M. Altaee, L.S. Cunningham, M. Gillie, Practical application of CFRP strengthening to steel floor beams with web openings: a numerical investigation, J. Constr. Steel Res. 155 (2019) 395–408.
[17] M.M. Kadhim, Z. Wu, L.S. Cunningham, Experimental and numerical investigation of CFRP-strengthened steel beams under impact load, J. Struct. Eng. 145 (4) (2019), 04019004.
[18] D.C. Kent, R. Park, Flexural members with confined concrete, J. Struct. Div. 97 (7) (1971) 1969–1990.
[19] ACI, Building Code Requirements for Structural Concrete (ACI 318-14) and Commentary (ACI 318R-14), American Concrete Inst, 2014.
[20] H.T. Nguyen, S.E. Kim, Finite element modeling of push-out tests for large stud shear connectors, J. Constr. Steel Res. 65 (10–11) (2009) 1909–1920.
[21] K. Fujikake, K. Mori, K. Uebayashi, T. Ohno, J. Mizuno, Constitutive model for concrete materials with high-rates of loading under tri-axial compressive stress states, in: Proceedings of the 3rd International Conference on Concrete under Severe Conditions, 2001, pp. 636–643.
[22] P. Symonds, Survey of Methods of Analysis for Plastic Deformation of Structures under Dynamic Loading, Brown University Providence, 1967. No. BU/NSRDC/1-67.
[23] N. Jones, Structural Impact, Cambridge University Press, Cambridge, 1997.
[24] Z. Hashin, Failure criteria for unidirectional fiber composites, J. Appl. Mech. 47 (2) (1980) 329–334.
[25] F. Dolce, Blast Impact Simulation on Composite Military Armours, University of Bath, 2009.
[26] M.M. Kadhim, Z. WuL, S. Cunningham, Numerical study of full-scale CFRP strengthened open-section steel columns under transverse impact, Thin-Walled Struct. 140 (2019) 99–113.
[27] Y.S. Muharrem Aktas, Nonlinear finite element analysis of damaged and strengthened Reinforced concrete beams, J. Civ. Eng. Manag. 20 (2) (2014) 201–210.
[28] X.Z. Lu, L.P. Ye, J.G. Teng, L.P. Ye, J.J. Jiang, Bond-slip models for FRP sheets/plates bonded to concrete, Eng. Struct. 27 (6) (2005) 920–937.
[29] A. Al-Mosawe, R. Al-Mahaidi, X.-L. Zhao, Experimental and numerical study on strengthening of steel members subjected to impact loading using ultrahigh modulus CFRP, J. Compos. Construct. 20 (6) (2016), 04016044.
[30] M.M. Kadhim, Z. Wu, L.S. Cunningham, Experimental study of CFRP strengthened steel columns subject to lateral impact loads, Compos. Struct. 185 (2018) 94–104.
[31] M. Zeinoddini, J. Harding, G. Parke, Axially pre-loaded steel tubes subjected to lateral impacts (a numerical simulation), Int. J. Impact Eng. 35 (11) (2008) 1267–1279.
[32] A. Genikomsou, A. Polak, Inite Element Analysis of RC Flat Slabs with Different Amount and Placement of Shear Bolts, ACI special publication, 2017, pp. 6.1–6.20. SP 321.
[33] M. Kadhim, Z. Wu, L. Cunningham, Modelling impact resistance of polymer-laminated steelwork, in: Proceedings of the Institution of Civil Engineers-Engineering and Computational Mechanics 170, 2017, pp. 7–24, 1.
[34] ACI-440.2, Guide for the Design and Construction of Externally Bonded FRP Systems for Strengthening Concrete Structures, American Concrete Institute, Farmington Hills, USA, 2002.